

**Optical shock and blow-up of ultrashort pulses in transparent media**P. Whalen,<sup>1</sup> J. V. Moloney,<sup>2,3,4</sup> A. C. Newell,<sup>3</sup> K. Newell,<sup>3</sup> and M. Kolesik<sup>2,4,5</sup><sup>1</sup>*Program in Applied Mathematics, University of Arizona, Tucson, AZ 85721-0089, USA*<sup>2</sup>*Arizona Center for Mathematical Sciences, University of Arizona, Tucson, AZ 85721-0089, USA*<sup>3</sup>*Department of Mathematics, University of Arizona, Tucson, AZ 85721-0089, USA*<sup>4</sup>*College of Optical Sciences, University of Arizona, Tucson, AZ 85721-0089, USA*<sup>5</sup>*Department of Physics, Constantine the Philosopher University, Nitra 94974, Slovakia*

(Received 30 January 2012; published 4 September 2012)

Ultrashort pulses can exhibit two distinctive types of singularity: self-focusing collapse and self-steepening shock. We examine various ultrashort pulse propagation models and their relative effectiveness in explaining these phenomena. In particular, the modified Kadomtsev-Petviashvili equation of type I (MKP1) is examined in some detail. We show that MKP1 is not simply a few-cycle pulse model but is valid in a more general broad spectrum setting. Furthermore, we emphasize that the dispersion of the MKP1 model can result in poor estimation of frequency-dependent phenomena, such as harmonic generation, which occur far away from the carrier frequency. Some of this loss of accuracy can be removed by using a more general MKP1 dispersion relation.

DOI: [10.1103/PhysRevA.86.033806](https://doi.org/10.1103/PhysRevA.86.033806)

PACS number(s): 42.65.Tg, 42.65.Jx, 42.65.Re

**I. INTRODUCTION**

Early theory on self-focusing and self-trapping of optical beams made extensive use of the nonlinear Schrödinger equation (NLSE) [1], with many results either motivated or confirmed by experimental observations [2]. However, the advent of ultrashort femtosecond lasers created a new range of phenomena that could not be explained by the NLSE: supercontinuum generation (SCG) [3], self-steepening shock [4], harmonics [5], etc. Newer technology, such as carrier-envelope offset phase-locked lasers [6], can produce pulse durations on the order of an optical cycle; current research efforts have centered on even shorter attosecond pulses [7]. The introduction of ultrashort propagation models [8–10] has led to a significantly better understanding of the underlying physics of such extremely short laser pulses.

This paper highlights three models that can propagate few-cycle pulses and exhibit both blow-up and shock singularity. Special attention is given to the modified Kadomtsev-Petviashvili equation of type I (MKP1) [8], which is as fundamental to optics in the ultrashort pulse regime as the NLSE is to optics in the longer pulse regime. Interestingly, much of the theory developed for critical power and self-similar collapse using the NLSE model [11] can be extended to the blow-up theory of ultrashort pulses using the MKP1 model [12]; specifically, singularities in both models can be analyzed either by utilizing their Hamiltonian structure or by performing self-similar transformations.

In broad spectral regimes, there is little extra cost in numerically resolving the details of a field compared with an envelope, and it becomes simple to add or remove harmonic generation and other field effects to a field model. This argument is frequently given by proponents of propagating the entire electric field rather than the envelope. On the other hand, the nonlinear envelope equations (NEE's) [9] can propagate both ultrashort pulses and long pulses, which makes them applicable over a wider range of problems. Another reason MKP1 and other full-field models such as the unidirectional pulse propagation equations (UPPE's) [10,12] have not been adopted as commonly as one might expect is

that historically, envelope models [13] have played a prominent role in nonlinear optics; building on an established theory is often preferential to the alternative of basing results on a newer or lesser known theory.

Since MKP1 is a focus of our paper, we note that it preceded both the NEE and UPPE models and that it has a well-established mathematical theory. Despite this, we find that the MKP1 is underutilized. Much of the literature on MKP1 focuses on few-cycle pulses [8,12,14,15], yet in this paper we simulate a self-focusing pulse with dozens of field oscillations under the envelope and show that MKP1 works well under these conditions. We also show that the generated harmonic fields [16–18] can be inaccurate due to the MKP1 dispersion approximation, and we show how to improve this accuracy.

**II. OPTICAL PROPAGATION MODELS**

Many important pulse propagation media such as air, water, or silica glass can be regarded as isotropic and homogeneous throughout. This considerably simplifies the constituent relations to Maxwell's equations and sets the groundwork necessary to reduce to a scalar propagation model. Assuming one-way propagation in the forward  $z$  direction by taking field reflections to be negligible is usually justified for high-power beams. Under these conditions, Maxwell's equations reduce to the most general first-order  $z$ -propagated optical model,

$$\partial_z E(k_\perp, z, \omega) = ik_z(\omega)E(k_\perp, z, \omega) + i \frac{\omega^2}{2\epsilon_0 c^2 k_z(k_\perp, \omega)} P_{\text{NL}}(k_\perp, z, \omega), \quad (1)$$

where  $E$  is the electric field,

$$k_z(\omega) = \sqrt{k^2(\omega) - k_\perp^2}$$

is the  $z$  component of the wave vector, and  $P_{\text{NL}}$  is the nonlinear polarization. From this unidirectional pulse propagation equation we can derive any first-order  $z$ -propagated model. Our study will focus on three of these models, which are used

in ultrashort pulse propagation: the UPPE model itself, the nonlinear envelope equations, and the MKP1 equation.

The UPPE model has the advantage of generality over both the NEE and MKP1 since the dispersion and nonlinear polarization have not assumed a specific form and the full electric field is propagated; using a specific medium model, prescribing a nonlinear response, or converting from a field equation to an envelope equation will put restrictions on what we can expect to accurately model in terms of the beam parameters and propagation environment. However, the gain in computational speed (NEE) and ease of analysis (MKP1) are compelling reasons to explore alternatives to the UPPE in certain settings.

To elucidate connections between the three models we derive NEE and MKP1 from the UPPE model. First, we mention that connections between Maxwell's equations, UPPE, NEE, and other models not including MKP1 are established in Ref. [10]. Connections between Maxwell's equations, MKP1, and NEE are established in Ref. [17]. Although much of the information in the remainder of this section can be found in these references along with Ref. [9], here we put a special emphasis on the role of dispersion in broad spectrum pulses. In particular, we clearly show that the dispersion approximations of the NEE and MKP1 models are valid over a limited spectral range; care must be taken when extrapolating results beyond this range.

When a beam width is on the order of a single optical wavelength, the transverse wave number  $k_{\perp}$  becomes quite large and the beam undergoes nonparaxial propagation. Feit and Fleck have shown that treating the wave number  $k_z$  in a nonparaxial manner, such as is done in the UPPE model, provides a mechanism for arresting catastrophic self-focusing collapse [19]. Often, high-power lasers will ionize a medium prior to reaching such an extremely narrow waist [20]. When this is the case, we make the paraxial propagation restriction  $k_{\perp} \ll |k|$  and expand out  $k_z$ :

$$k_z(\omega) \approx k(\omega) - \frac{k_{\perp}^2}{2k(\omega)}. \quad (2)$$

Supposing the medium nonlinearity is sufficiently weak [the second right-hand side term in Eq. (1) is much smaller than the first], then a paraxial beam implies

$$\frac{\omega^2}{2\epsilon_0 c^2 k_z(k_{\perp}, \omega)} P_{\text{NL}} \approx \frac{\omega^2}{2\epsilon_0 c^2 k(\omega)} P_{\text{NL}}.$$

After some manipulations,

$$\partial_z E(k_{\perp}, z, \omega) = ik(\omega)E - \frac{ick_{\perp}^2}{2n(\omega)\omega} E + \frac{i\omega}{2\epsilon_0 cn(\omega)} P_{\text{NL}}. \quad (3)$$

Both the NEE and MKP1 make use of a central or reference frequency of the pulse. Typically the reference frequency is taken to be the carrier frequency at which the beam is driven. However, during propagation the spectral peak may move away from the chosen reference frequency; in fact, when pulse splitting occurs, two distinct spectral peaks can form, neither of which is at the carrier frequency of the pulse [21]. It is easy to think of other situations where the concept of a central frequency may become ambiguous: third harmonic (TH) generation, supercontinuum generation, colliding pulses with differing center frequencies, etc. Having a spectral peak

away from the reference frequency is concerning, but it does not necessarily mean the model is inaccurate. Assuming a reference frequency  $\omega_R$  and Taylor expanding the two  $n^{-1}(\omega)$  terms in Eq. (3) yields

$$\begin{aligned} \partial_z E(k_{\perp}, z, \omega) &= ik(\omega)E - \frac{ick_{\perp}^2}{2n(\omega_R)\omega} \left[ 1 - \frac{n'(\omega_R)(\omega - \omega_R)}{n(\omega_R)} + \dots \right] E \\ &+ \frac{i\omega}{2\epsilon_0 cn(\omega_R)} \left[ 1 - \frac{n'(\omega_R)(\omega - \omega_R)}{n(\omega_R)} + \dots \right] P_{\text{NL}}. \end{aligned} \quad (4)$$

A sufficiently well-behaved linear medium response will satisfy

$$|n'(\omega_R)\omega_R| \ll n(\omega_R),$$

which is one of two explicit conditions necessary for the NEE to be valid [9]. When considered with the other necessary condition, Brabec and Krausz coined this the slowly evolving wave approximation. The second condition concerns an envelope and is not explicitly needed for the MKP1 model. Both the NEE and MKP1 have a dispersion relation which is only valid in the transparent region, well below resonant frequencies and well above the plasma frequency. With this additional restriction we have

$$\partial_z E(k_{\perp}, z, \omega) = ik(\omega)E - \frac{ick_{\perp}^2}{2n(\omega_R)\omega} E + \frac{i\omega}{2\epsilon_0 cn(\omega_R)} P_{\text{NL}}, \quad (5)$$

a model that captures most optical mediums and realistic beam parameters.

The dispersion relations for the MKP1 and NEE models are given by

$$\begin{aligned} k_{\text{MKP1}}(\omega) &= a\omega^3 - \frac{b}{\omega} + q\omega, \\ k_{\text{NEE}}(\omega) &= \sum_{m=0}^{\infty} \frac{k^{(m)}(\omega_R)}{m!} (\omega - \omega_R)^m. \end{aligned}$$

For a better MKP1 dispersion approximation we can use the generalized dispersion relation

$$k_{\text{GMKP1}}(\omega) = \sum_{m=0}^{\infty} a_{2m+1} \omega^{2m+1} - \sum_{n=0}^{\infty} b_{2n+1} \omega^{-2n-1}. \quad (6)$$

More details on the generalized MKP1 model are available in Ref. [16]. Even with the additional terms, the MKP1 dispersion and the NEE dispersion are the weakest links in the approximations to the general UPPE equation. This is particularly true for few-cycle and broad spectrum pulses [22].

For fused silica, the UPPE dispersion consists of a Sellmeier formula. An 800-nm pulse generates MKP1 and NEE dispersion parameters of  $a = 3.1 \times 10^{-42} \text{ s}^3/\text{m}$ ,  $b = 4.0 \times 10^{19} \text{ s}^{-1}/\text{m}$ ,  $k_2 = 3.6 \times 10^{-26} \text{ s}^2/\text{m}$ , and  $k_3 = 2.8 \times 10^{-41} \text{ s}^3/\text{m}$ , respectively. It can be seen that the dispersion approximations are nearly identical around the carrier frequency  $\omega_0$  (Fig. 1). Close to the third harmonic, the index of refraction of the UPPE and MKP1 models are similar but the GVD is nearly twice as large in the UPPE model as it is in the MKP1 model. Adding an  $a_5$  term to the MKP1 dispersion does a good job of removing this discrepancy in the GVD.

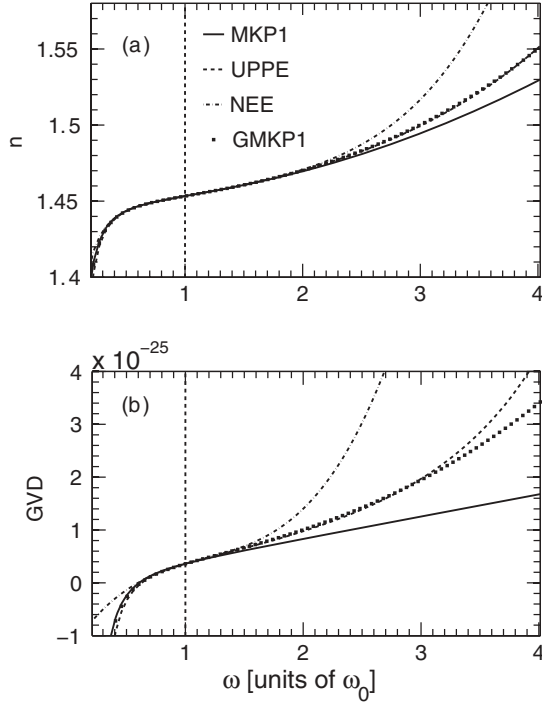


FIG. 1. (a) Fused silica index of refraction (b) and group velocity dispersion. GVD corresponds to the second derivative  $d^2k/d\omega^2$  of the respective dispersion models.

For the GMKP1 model we compute  $a_3 = 2.77 \times 10^{-42} \text{ s}^3/\text{m}$ ,  $a_5 = 1.1 \times 10^{-74} \text{ s}^5/\text{m}$ , and  $b_1 = 3.9 \times 10^{19} \text{ s}^{-1}/\text{m}$ . As we show in Sec. IV, accurate resolution of the third harmonic will require the better fit of the GMKP1 dispersion relation.

After substituting the MKP1 dispersion relation into Eq. (5) and transforming to time-domain real space, the MKP1 model becomes

$$\partial_\tau \left( \partial_z E - a \partial_\tau^3 E + \frac{1}{2\epsilon_0 c n(\omega_R)} \partial_\tau P_{\text{NL}} \right) + b E = \frac{c}{2n(\omega_R)} \Delta_\perp E, \quad (7)$$

where  $\tau = t - qz$ . The  $a$  and  $b$  terms correspond to the linear electronic and vibrational polarizations of the medium, respectively. It should be noted that the change of variable puts the system into a moving reference frame that does not necessarily coincide with the group velocity of the pulse.

To obtain the NEE, we assume

$$E(x_\perp, z, t) = \mathcal{E}(x_\perp, z, t) e^{ik(\omega_R)z - i\omega_R t} + \text{c.c.},$$

$$P_{\text{NL}}(x_\perp, z, t) = h(|\mathcal{E}|) \mathcal{E}(x_\perp, z, t) e^{ik(\omega_R)z - i\omega_R t} + \text{c.c.},$$

where  $\mathcal{E}$  is an envelope and  $h$  is a function corresponding to the nonlinear response of the medium. After substituting the NEE envelope and dispersion parameters into (5), and assuming a sufficiently narrow spectrum, the spectral NEE is given as

$$\partial_z \mathcal{E}(k_\perp, z, \Omega) = i \sum_{m=1} \frac{k^{(m)}(\omega_R)}{m!} \Omega^m \mathcal{E} - \frac{ick_\perp^2}{2n(\omega_R)(\Omega + \omega_R)} \mathcal{E} + \frac{i(\Omega + \omega_R)}{2\epsilon_0 c n(\omega_R)} \mathcal{F}\{h(|\mathcal{E}|)\mathcal{E}\}, \quad (8)$$

where  $\Omega = \omega - \omega_R$  and  $\mathcal{F}$  denotes a Fourier transform. Converting to a time-domain real-space equation, we obtain

$$\begin{aligned} (\partial_z + v_g^{-1} \partial_t) \mathcal{E}(x_\perp, z, t) &= \frac{i}{2k(\omega_R)} \left( 1 + \frac{i}{\omega_R} \partial_t \right)^{-1} \Delta_\perp \mathcal{E} + D(i\partial_t) \mathcal{E} \\ &+ \frac{ik(\omega_R)}{2\epsilon_0 n(\omega_R)^2} \left( 1 + \frac{i}{\omega_R} \partial_t \right) h(|\mathcal{E}|) \mathcal{E}, \end{aligned} \quad (9)$$

where  $v_g^{-1} = k'(\omega_R)$  is the group velocity and the dispersion operator is

$$D(i\partial_t) = \sum_{m=2} \frac{k^{(m)}(\omega_R)}{m!} (i\partial_t)^m.$$

There are two types of nonlinear effects that can compete: nonlinear polarization, which causes a sufficiently powered beam to undergo self-focusing collapse, and ionization, which arrests collapse and prevents singularity formation. Since shock formation and blow-up can occur with or without medium ionization, we leave plasma defocusing out of our equations and acknowledge that an important term that often acts to regularize singularities is missing.

Another approximation we will make is to assume an instantaneous nonlinear response of the electric field. In Secs. III and IV we simulate beams with pulse widths of 50 fs and 1.8 fs, respectively. The noninstantaneous Raman effect of the 1.8-fs pulse should be negligible, but we would expect some Raman response in the 50-fs case. However, unlike plasma effects, the Raman effect is not expected to play a significant role in the singularity dynamics of the system, and we disregard it in our simulations.

To incorporate harmonic effects into our full-field MKP1 and UPPE propagators we use the nonlinear response function

$$P_{\text{NL}}(x_\perp, z, t) = \frac{4}{3} \epsilon_0 n(\omega_0) n_2 E^3(x_\perp, z, t), \quad (10)$$

where  $n_2$  is the Kerr nonlinear index of refraction. This response will generate third and higher harmonic pulses. Typically, the fundamental pulse is only weakly affected by the harmonic signals it generates. If this is the case, and resolving the harmonic signals themselves is not important to us, then we can remove the harmonic signals by replacing Eq. (10) with an NEE formulation of the nonlinear response:

$$P_{\text{NL}}(x_\perp, z, t) = 2\epsilon_0 n(\omega_0) n_2 |E|^2 E(x_\perp, z, t).$$

Alternatively, we can propagate spectral components that reside between a range  $(\omega_{\text{min}}, \omega_{\text{max}})$  and zero out unwanted frequency content. Using this method we set  $\omega_{\text{max}} < 3\omega_0$  such that the third harmonic and higher harmonic frequencies are not propagated along with the fundamental pulse. Unless otherwise stated, this will be the method used to turn off harmonic generation in simulations of the MKP1 and UPPE field models.

While the NEE and UPPE can incorporate many kinds of nonlinear response, the MKP1 model specifically uses a cubic field term such as in Eq. (10). Therefore, we explicitly plug

this into Eq. (7) to obtain

$$\partial_\tau \left( \partial_z E + \frac{2n_2}{c} E^2 \partial_\tau E - a \partial_\tau^3 E \right) + bE = \frac{c}{2n(\omega_R)} \Delta_\perp E. \quad (11)$$

This is MKP1 to within some nondimensional scalings. Various generalizations of this model have been made. One generalization already mentioned incorporates a better dispersion model. Another generalization models a circularly polarized field [14]. In this paper we only consider linearly polarized electric fields.

### III. BLOW-UP

Conventionally, when studying singularities the equation of interest is first nondimensionalized. Here we rescale the variables in the MKP1 model such that  $\tilde{E} = \sqrt{\frac{8L_{DF}}{3L_{NL}}} \frac{E}{\sqrt{I_0}}$ ,  $\tilde{\tau} = \omega_R \tau$ ,  $\tilde{r} = \frac{r}{w_0}$ ,  $\tilde{z} = \frac{z}{4L_{DF}}$ , where  $I_0$  is the input field intensity,  $w_0$  is the initial beam diameter,  $L_{DF}$  is the diffractive length scale, and  $L_{NL}$  is the nonlinear length scale

$$L_{DF} = \frac{k(\omega_R)w_0^2}{2}, \quad L_{NL} = \frac{c}{\omega_R n_2 I_0}. \quad (12)$$

Substituting into (11), then dropping the tildes for convenience, will yield

$$\partial_\tau (\partial_z E + 3E^2 \partial_\tau E - A \partial_\tau^3 E) + BE = \Delta_\perp E, \quad (13)$$

with  $A$  and  $B$  defined as

$$A = \frac{L_{DF}}{L_{ds,H}}, \quad B = \frac{L_{DF}}{L_{ds,L}}.$$

The length scales  $L_{DF}$  and  $L_{NL}$  have standard nonlinear optics meanings [13] and are often used in conjunction with an initial Gaussian pulse of the form

$$E(r,0,t) = \sqrt{I_0} \exp \left[ -\frac{t^2}{t_p^2} - \frac{r^2}{w_0^2} - i\omega_R t \right] + \text{c.c.} \quad (14)$$

On the other hand, nonconventional dispersion length scales

$$L_{ds,L} = \frac{\omega_R}{4b}, \quad L_{ds,H} = \frac{1}{4a\omega_R^3}, \quad (15)$$

are produced when nondimensionalizing in this manner. The  $L_{ds,L}$  scale comes from low-frequency plasma effects and  $L_{ds,H}$  corresponds to high-frequency dispersion. Traditional length scales are given by

$$L_{DS} = \frac{t_p^2}{2k''(\omega_R)}, \quad L'_{DS} = \frac{t_p^3}{k'''(\omega_R)}, \quad (16)$$

which correspond to second- and third-order dispersion in the NLSE and NEE envelope models.

Critical power is an important concept when analyzing the blow-up singularity. When a beam input power becomes greater than a certain threshold ( $P_{in} > P_{th}$ ), then nonlinear focusing overcomes diffraction, dispersion, and other defocusing forces and the beam diameter begins to shrink. This process feeds on itself by creating an ever more intense beam core, hence stronger nonlinear focusing. Often diffraction is the largest defocusing effect, so the power needed to overcome it has special significance and is referred to as critical power.

Critical power can be associated with the Hamiltonian of the NLSE system [23], and there is a similar connection to the MKP1 model [12]. For convenience, a potential function  $E = \Phi_\tau$  is introduced. Then the wave action, Lagrangian, and Hamiltonian of (13) are given by

$$N = \int \Phi_\tau^2 d\tau dx_\perp, \quad (17)$$

$$L = \frac{1}{2} \Phi_z \Phi_\tau + \frac{\Phi_\tau^4}{4} + \frac{A}{2} \Phi_{\tau\tau}^2 - \frac{1}{2} (\nabla_\perp \Phi)^2 - \frac{B}{2} \Phi^2, \quad (18)$$

$$H = \int \left[ (\nabla_\perp \Phi)^2 - \frac{\Phi_\tau^4}{2} - A \Phi_{\tau\tau}^2 + B \Phi^2 \right] d\tau dx_\perp. \quad (19)$$

Using the method of moments, a relationship for the transverse waist of the beam can be expressed as

$$\frac{d^2 w_{\text{eff}}^2}{dz^2} = \frac{8H + 8 \int [A \Phi_{\tau\tau}^2 - B \Phi^2] d\tau dx_\perp}{N}, \quad (20)$$

where

$$w_{\text{eff}}^2 = \frac{\int x_\perp^2 \Phi_\tau^2 d\tau dx_\perp}{N}.$$

When the right-hand side of (20) is negative, the transverse beam diameter shrinks and the beam is in a collapsing state. Since the quantity

$$A \Phi_{\tau\tau}^2 - B \Phi^2$$

is nonconserved, there are no guarantees that a beam in a collapsing state will stay in a collapsing state unless the conditions  $H < 0$  and  $A = 0$  are satisfied. Noting that

$$k''_{\text{MKP1}}(\omega) = \frac{1}{2L_{DF}\omega_R^2} \left( \frac{\omega}{\omega_R} \right) \left[ 3A - B \left( \frac{\omega}{\omega_R} \right)^2 \right]$$

we see that the condition  $A = 0$  corresponds to the anomalous dispersion regime. However, it should be noted that anomalous dispersion does not imply that  $A = 0$  and setting  $A = 0$  will typically result in a dispersive medium that is not physically realizable. Furthermore, the dispersion approximation will become particularly bad over a large spectral range and a collapsing pulse generates a broad spectrum. That is, we need  $A = 0$  to guarantee a mathematical blow-up singularity, yet by setting  $A = 0$  the model is no longer accurate for pulses collapsing in a dispersive media. In terms of guaranteed collapse behavior, Eq. (20) does not tell us much. We can make some important qualitative observations, however. Regardless of whether the dispersion is anomalous or normal, having a negative Hamiltonian will make the system more susceptible to collapse. If we consider a normally dispersive medium with  $H < 0$  and

$$|H| \gg \int [A \Phi_{\tau\tau}^2 - B \Phi^2] d\tau dx_\perp,$$

then conceivably the field amplitude can grow significantly before the  $A \Phi_{\tau\tau}^2$  term begins to dominate and collapse is arrested. Another observation comes from the fact that

$$\phi_\tau^4 \sim \left( \frac{L_{DF}}{L_{NL}} \right)^2.$$

Consequently, increasing the beam intensity of the initial pulse will reduce the Hamiltonian and enhance the likelihood of blow-up.



Suppose the medium is nondispersive and the electric field takes a scalar monochromatic form

$$E(x_{\perp}, z, t) = \frac{\mathcal{E}(x_{\perp}, z)e^{ik(\omega_R)z - i\omega_R t} + \text{c.c.}}{2}.$$

Then, in our transformed variables,

$$\tilde{E}(\tilde{x}_{\perp}, \tilde{z}, \tilde{t}) = \frac{\tilde{\mathcal{E}}(\tilde{x}_{\perp}, \tilde{z})e^{-i\tilde{t}} + \text{c.c.}}{2}, \quad (21)$$

$$\partial_{\tilde{t}} \tilde{E} = \frac{-i\tilde{\mathcal{E}}e^{-i\tilde{t}} + \text{c.c.}}{2}, \quad (22)$$

$$\phi = \frac{i\tilde{E}e^{-i\tilde{t}} + \text{c.c.}}{2}. \quad (23)$$

The MKP1 model reduces to the time-independent NLSE when the dispersion terms are dropped, and the nonlinear polarization is altered to be proportional to  $|E|^2$  rather than  $E^3$ . Scalings in the nondimensional NLSE model are generally chosen different than in the nondimensional MKP1. By rescaling  $\tilde{E}$  such that

$$\tilde{E} = \sqrt{\frac{2L_{\text{DF}}}{L_{\text{NL}}}} \frac{E}{\sqrt{I_0}}$$

and dropping dispersive terms, the MKP1 model becomes

$$\partial_{\tilde{t}} (\partial_{\tilde{z}} \tilde{E} + \frac{4}{3} \partial_{\tilde{t}} \tilde{E}^3) = \tilde{\Delta}_{\perp} \tilde{E}. \quad (24)$$

Substituting (21) into the previous equation and ignoring third harmonic terms yields the nondimensional NLSE

$$i\partial_z \mathcal{E} + |\mathcal{E}|^2 \mathcal{E} + \Delta_{\perp} \mathcal{E} = 0, \quad (25)$$

where the tildes have been removed after substitution. Under these conditions the corresponding NLSE action integral, Lagrangian, and Hamiltonian are

$$N = \frac{1}{2} \int |\mathcal{E}|^2 dx_{\perp}, \quad (26)$$

$$L = \frac{1}{8} [i\mathcal{E}_z \mathcal{E}^* - i\mathcal{E}^* \mathcal{E}_z] + \frac{|\mathcal{E}|^4}{8} - \frac{1}{4} |\nabla_{\perp} \mathcal{E}|^2, \quad (27)$$

$$H = \frac{1}{2} \int \left[ |\nabla_{\perp} \mathcal{E}|^2 - \frac{|\mathcal{E}|^4}{2} \right] dx_{\perp}, \quad (28)$$

where again the tildes are removed after substitutions. For the NLSE case, an initial Hamiltonian being negative assures us the solution blows up. However, the minimum power required for blow-up has more to do with the Townes beam than the sign of the Hamiltonian [24]. Different beam geometries have different critical powers. In particular, a Gaussian beam has the critical power

$$P_{\text{cr}} = \frac{3.77\lambda_0^2}{8\pi n_0 n_2}.$$

Threshold power for collapse can be noticeably larger than critical power due to dispersion.

For a Gaussian beam of pulse width  $t_p = 50$  fs, diameter  $w_0 = 30 \mu\text{m}$ , and intensity  $I_0 = 2.7 \times 10^{15} \text{ W/m}^2$ , blow-up is simulated in silica glass (Fig. 2). The laser is run at  $\lambda_0 = 800$  nm with an input power modestly above critical power,  $P_{\text{in}} = 1.74P_{\text{cr}}$ . The nonlinear index of refraction is set to  $n_2 = 3.0 \times 10^{-20} \text{ m}^2/\text{W}$  and the reference frequency is selected equal to the carrier frequency  $\omega_R = \omega_0$ . All three

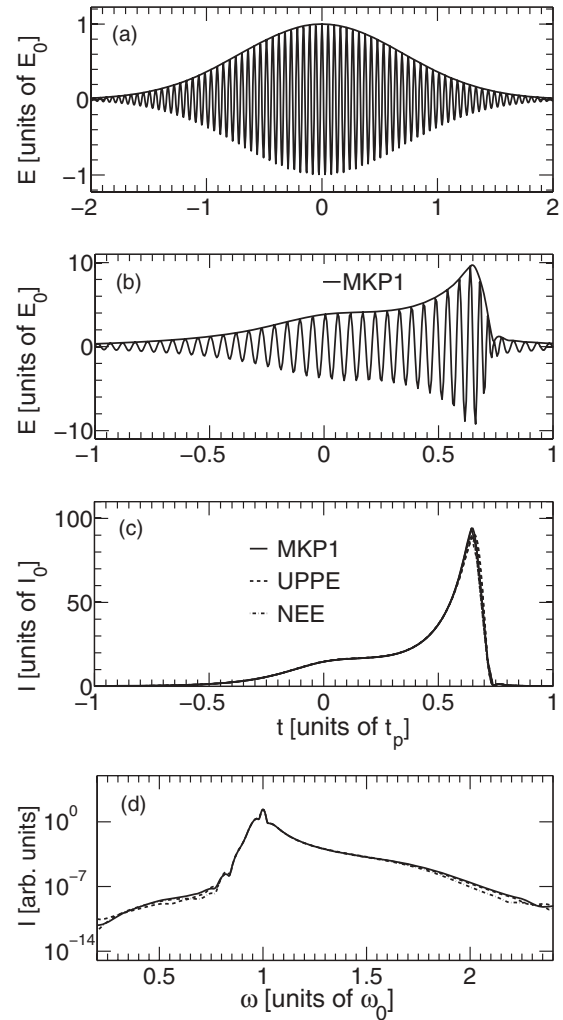


FIG. 2. Self-focusing collapse in fused silica with initial field  $E_0 = \sqrt{I_0} \exp(-t^2/t_p^2 - r^2/w_0^2 - i\omega_0 t) + \text{c.c.}$  and parameters  $t_p = 50$  fs,  $w_0 = 30 \mu\text{m}$ , and  $I_0 = 2.7 \times 10^{15} \text{ W/m}^2$ . On-axis field and envelope at (a)  $z = 0$  mm and (b)  $z = 4.93$  mm. (c) On-axis intensity at  $z = 4.93$  mm. (d) On-axis spectrum at  $z = 4.93$  mm.

models are propagated using an ODE45 solver and assume radial symmetry in the transverse dimension. For the blow-up simulations, harmonic generation is effectively ignored by setting the maximum frequency propagated to  $\omega_{\text{max}} = 2.55\omega_0$ .

Shown in Fig. 2(a) is the initial field profile. Once propagation is initiated, self-focusing causes the beam diameter and pulse width to shrink. Figure 2(b) illustrates the temporal compression of the beam, which coincides with a steepening of the pulse toward the tail [4]. Collapse is arrested shortly afterward by pulse splitting [21]. The narrowing pulse width is also associated with spectral broadening. Most of the broadening occurs for frequencies above the carrier, an effect observed experimentally during supercontinuum generation [25].

A comparison is made between the MKP1, UPPE, and NEE models in Figs. 2(c) and 2(d). Clearly, differences in the simulation results are insignificant. To some extent, which model to pick becomes a matter of preference. We do point out a few important details, however. First, the UPPE model is not well suited for analysis compared with the NEE and MKP1

models. Second, if during propagation the spectrum must be resolved over a frequency range  $\sim \omega_R$ , then there is little to no computational advantage for using an envelope model such as NEE as compared with a field model such as MKP1 or UPPE.

We want to emphasize that while a 50-fs pulse is considered ultrashort, there are more than a few carrier oscillations under the envelope. We also note that for these pulse parameters, the beam self-focuses until the pulse intensity is about 100 times the initial intensity. Self-focusing of a pulse with only a couple of cycles under the envelope induces relatively little blow-up. Much of the literature on the MKP1 model highlights its use in the few-cycle pulse regime. A more encapsulating description of when the MKP1 is useful is in the extremely broad spectral regime. This regime can include pulses that initially have a narrow spectrum but broaden significantly during propagation, as is true in our self-focusing blow-up case.

#### IV. SHOCK

The theory of shocks in physical settings has been well established [26]. Here, we give an explanation of what causes

a shock in ultrashort optical pulses using MKP1 as an analytic tool. First take a constant index of refraction  $n_0$  and assume diffraction is negligible. Then, in the stationary reference frame, the MKP1 model will take the form

$$\partial_z E + \frac{2n_2}{c} E^2 \partial_t E + \frac{n_0}{c} \partial_t E = 0.$$

Considering characteristic curves in the  $(t, z)$  plane

$$\frac{dE}{dz} = \partial_z E + \frac{dt}{dz} \partial_t E = 0,$$

we find

$$\frac{dt}{dz} = \frac{n_0 + 2n_2 E^2}{c}.$$

Normalizing the electric field to intensity and time averaging yields

$$\frac{dz}{dt} = \frac{c}{n_0 + n_2 I}. \quad (29)$$

Along any given characteristic line in the  $(t, z)$  plane, the field  $E$  and hence intensity  $I$  and speed  $\frac{dz}{dt}$  are constants. For

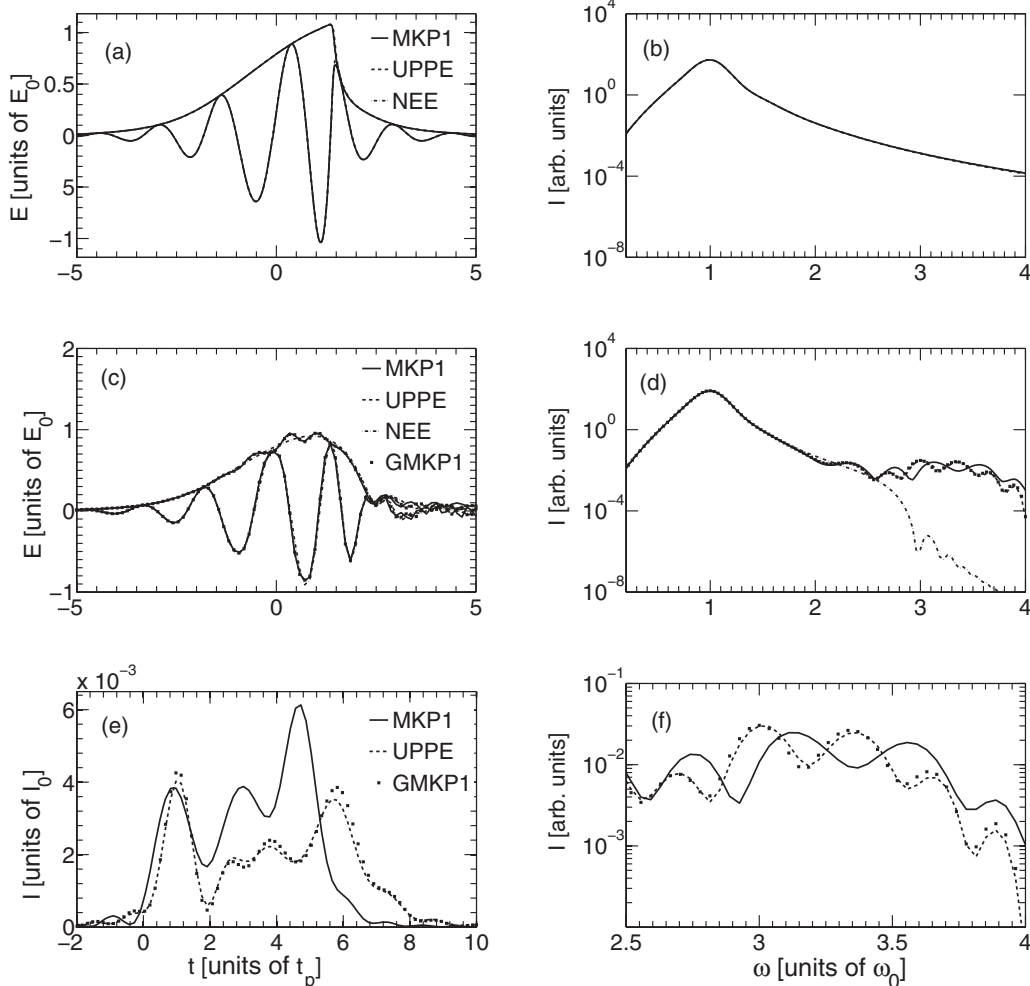


FIG. 3. Self-steepening shock in fused silica with initial field  $E_0 = \sqrt{I_0} \text{sech}(t/t_p) \exp(-r^2/w_0^2 - i\omega_0 t) + \text{c.c.}$  and parameters  $I_0 = 5.0 \times 10^{17} \text{ W/m}^2$ ,  $t_p = 1.8 \text{ fs}$ , and  $w_0 = 10 \mu\text{m}$ . In each figure the pulse propagated  $14.9 \mu\text{m}$ . Constant index of refraction  $n_0 = 1.45$  and no harmonic generation: field (a) and spectrum (b). Index of refraction  $n(\omega)$  as shown in Fig. 1 and third harmonic generation: field (c), spectrum (d), third harmonic temporal profile (e), and frequency content of third harmonic (f).

a Gaussian or hyperbolic secant initial pulse there is a central peak with a decaying intensity as a function of distance from the temporal center. Equation (29) shows that the center of the pulse will follow a characteristic line traveling slower than the front or tail of the pulse. As a consequence, energy from the temporal center moves toward the tail, causing a steep edge and optical shock. Energy in the front has a lower intensity and travels faster than the peak of the wave front.

Consider a pulse propagated in fused silica at an optical wavelength of 800 nm. For an initial field  $E_0 = \sqrt{I_0} \text{sech}(t/t_p) \exp(-r^2/w_0^2 - i\omega_0 t) + \text{c.c.}$ , with  $I_0 = 5.0 \times 10^{17} \text{ W/m}^2$ ,  $w_0 = 10.0 \mu\text{m}$ , and  $t_p = 1.8 \text{ fs}$ , nonlinear effects are relatively strong while diffraction is almost negligible. To illustrate shock, harmonic generation is ignored and simulations are run with a constant index of refraction. The amount of steepening that can be obtained is increased by using an NEE nonlinear polarization response ( $\sim |E|^2 E$ ) in the field MKP1 and UPPE models. This enables us to propagate frequencies larger than  $3\omega_0$  without having harmonic effects enter the simulation. After propagating  $14.9 \mu\text{m}$ , a large temporal gradient emerges at the tail of the pulse as shown in Fig. 3(a).

It should be noted that we have illustrated an “envelope shock.” Both the UPPE and MKP1 can also undergo a “field shock,” which corresponds to a steepening of the carrier wave and a field profile that resembles a trapezoidal shape [27]. A field shock is caused by a cascading of odd harmonics due to a full-field nonlinear response ( $\sim E^3$ ) and is strongest in a nondispersive media. Similar to an envelope shock, dispersion tends to regularize the amount of steepening that occurs in a field shock.

When dispersion and a full-field nonlinear response are taken into account, self-steepening occurs but to a much lesser extent [Fig. 3(c)]. Dispersion is relatively weak compared to nonlinearity  $L_{\text{NL}}/L_{\text{DS}} = 0.19$  but clearly arrests an optical shock from forming. A self-steepening length scale is given by  $L_{\text{ss}} = L_{\text{NL}}\omega_R t_p$  [28]. Generally  $L_{\text{NL}} \ll L_{\text{ss}}$ , but in our case the pulse is extremely short such that  $L_{\text{ss}} = 4.2L_{\text{NL}}$ . On the other hand,  $L_{\text{ss}} = 0.80L_{\text{DS}}$  and a decent amount of dispersion will happen before the pulse travels a shock distance of  $L_{\text{ss}}$ .

Third harmonic effects are small compared to the main pulse, which makes them hard to distinguish in the temporal domain. However, they make the envelope slightly oscillatory, and if we look at the spectrum in Fig. 3(d), TH generation becomes easy to observe. Figure 3(f) zooms in on what we will consider the TH spectral content of the MKP1, UPPE, and GMKP1 field models. Taking the inverse Fourier transform of the TH spectral content with the remaining spectrum set to zero produces the TH temporal profile shown in Fig. 3(f).

The multiple peaks can be attributed to TH pulse splitting. Farthest on the left is a temporal peak that travels along with the fundamental field. The other peaks correspond to parts of the TH pulse that split off and lag behind the main pulse.

From Figs. 3(e) and 3(f) we notice that the UPPE and GMKP1 models produce nearly identical TH effects while the MKP1 model predicts noticeably different TH effects. This can be attributed to the differences in the dispersion approximations of the MKP1 and GMKP1 models. MKP1 cannot approximate the Sellmeier formula for fused silica accurately enough at the third harmonic, but by adding additional terms as is done in the GMKP1 model we get a better fit farther away from the carrier frequency and much more accurate at the third harmonic.

## V. CONCLUSIONS

Optical shock and self-focusing blow-up are two fundamental singularities of great interest in nonlinear optics. Early theory and experimental work on singularities in optics focused mainly on blow-up, but newer work in the ultrashort pulse regime has emphasized the role of self-steepening and shock. While NLSE theory and its connection to optics has been thoroughly developed, a fuller understanding of singularity formation of short pulses requires a more accurate model. In this paper, we have illustrated three equations used in ultrashort pulse propagation with an emphasis on the MKP1 model and its usefulness as an analytic tool.

We have shown that the restriction of MKP1 to few-cycle pulses is unnecessary. Even when a few dozen cycles are under the envelope, MKP1 can be as effective as the NEE and UPPE in simulating self-focusing ultrashort femtosecond pulses. In general, MKP1 can be an effective model for any system in which a large spectral range must be propagated.

Commonly, MKP1 and other field models include effects such as third harmonic generation. Accurately resolving a third harmonic field requires propagating with a dispersion model that is accurate at the third harmonic frequency. MKP1 dispersion can fail in this context, and it may be necessary to use a more general dispersion expansion. Furthermore, if no analysis of the model is needed, it may be best to simply stay in the spectral domain and simulate using a model with an exact dispersion relation such as UPPE.

## ACKNOWLEDGMENTS

The authors wish to acknowledge funding support through Multidisciplinary University Research Initiative (MURI) Grant No. AFOSR FA9550-10-1-0561.

- 
- [1] V. Talanov, *JETP Lett.* **2**, 138 (1965); P. L. Kelley, *Phys. Rev. Lett.* **15**, 1005 (1965); R. Y. Chiao, E. Garmire, and C. H. Townes, *ibid.* **13**, 479 (1964); J. H. Marburger, *Prog. Quantum Electron.* **4** (Part 1), 35 (1975).  
 [2] Y. R. Shen, *Prog. Quantum Electron.* **4** (Part 1), 1 (1975).  
 [3] A. Brodeur and S. L. Chin, *J. Opt. Soc. Am. B* **16**, 637 (1999).

- [4] A. L. Gaeta, *Phys. Rev. Lett.* **84**, 3582 (2000).  
 [5] M. Kolesik, E. Wright, A. Becker, and J. Moloney, *Appl. Phys. B* **85**, 531 (2006).  
 [6] C. Hauri, W. Kornelis, F. Helbing, A. Heinrich, A. Couairon, A. Mysyrowicz, J. Biegert, and U. Keller, *Appl. Phys. B* **79**, 673 (2004).

- [7] G. Sansone, E. Benedetti, F. Calegari, C. Vozzi, L. Avaldi, R. Flammini, L. Poletto, P. Villoresi, C. Altucci, R. Velotta, S. Stagira, S. De Silvestri, and M. Nisoli, *Science* **314**, 443 (2006), <http://www.sciencemag.org/content/314/5798/443.full.pdf>.
- [8] S. Kozlov and S. Sazonov, *J. Exp. Theor. Phys.* **84**, 221 (1997).
- [9] T. Brabec and F. Krausz, *Rev. Mod. Phys.* **72**, 545 (2000).
- [10] M. Kolesik and J. V. Moloney, *Phys. Rev. E* **70**, 036604 (2004).
- [11] J. J. Rasmussen and K. Rypdal, *Phys. Scr.* **33**, 481 (1986); K. Rypdal and J. J. Rasmussen, *ibid.* **33**, 498 (1986).
- [12] A. Balakin, A. Litvak, V. Mironov, and S. Skobelev, *J. Exp. Theor. Phys.* **104**, 363 (2007); M. Kolesik, J. V. Moloney, and M. Mlejnek, *Phys. Rev. Lett.* **89**, 283902 (2002).
- [13] A. Couairon and A. Mysyrowicz, *Phys. Rep.* **441**, 47 (2007).
- [14] A. A. Balakin, A. G. Litvak, V. A. Mironov, and S. A. Skobelev, *Phys. Rev. A* **78**, 061803 (2008).
- [15] A. A. Balakin, A. G. Litvak, V. A. Mironov, and S. A. Skobelev, *Phys. Rev. A* **80**, 063807 (2009).
- [16] V. G. Bespalov, S. A. Kozlov, Y. A. Shpolyanskiy, and I. A. Walmsley, *Phys. Rev. A* **66**, 013811 (2002).
- [17] A. N. Berkovsky, S. A. Kozlov, and Y. A. Shpolyanskiy, *Phys. Rev. A* **72**, 043821 (2005).
- [18] K. Glasner, M. Kolesik, J. Moloney, and A. Newell, *International Journal of Optics* **2012**, 868274 (2012).
- [19] M. D. Feit and J. J. A. Fleck, *J. Opt. Soc. Am. B* **5**, 633 (1988).
- [20] E. Yablonovitch and N. Bloembergen, *Phys. Rev. Lett.* **29**, 907 (1972); A. Braun, G. Korn, X. Liu, D. Du, J. Squier, and G. Mourou, *Opt. Lett.* **20**, 73 (1995); Y. P. Deng, J. B. Zhu, Z. G. Ji, J. S. Liu, B. Shuai, R. X. Li, Z. Z. Xu, F. Théberge, and S. L. Chin, *ibid.* **31**, 546 (2006).
- [21] J. E. Rothenberg, *Opt. Lett.* **17**, 1340 (1992); P. Chernev and V. Petrov, *ibid.* **17**, 172 (1992).
- [22] K. E. Oughstun and H. Xiao, *Phys. Rev. Lett.* **78**, 642 (1997).
- [23] G. Fibich and A. L. Gaeta, *Opt. Lett.* **25**, 335 (2000).
- [24] K. D. Moll, A. L. Gaeta, and G. Fibich, *Phys. Rev. Lett.* **90**, 203902 (2003).
- [25] W. M. Wood, C. W. Siders, and M. C. Downer, *Phys. Rev. Lett.* **67**, 3523 (1991).
- [26] A. V. Gaponov, L. A. Ostrovskii, and G. I. Freidman, *Radiophys. Quantum Electron.* **10**, 772 (1967); G. Whitham, *Linear and Nonlinear Waves* (Wiley, New York, 1974).
- [27] R. G. Flesch, A. Pushkarev, and J. V. Moloney, *Phys. Rev. Lett.* **76**, 2488 (1996); A. Litvak, V. Mironov, and S. Skobelev, *JETP Lett.* **82**, 105 (2005); G. Genty, P. Kinsler, B. Kibler, and J. M. Dudley, *Opt. Express* **15**, 5382 (2007).
- [28] R. W. Boyd, *Nonlinear Optics*, 3rd ed. (Academic, New York, 2008).